ACS ENGINEERING Au
AN OPEN ACCESS JOURNAL OF THE AMERICAN CHEMICAL SOCIETY

pubs.acs.org/engineeringau

Letter

Thermochromic Fenestration Elements Based on the Dispersion of Functionalized VO_2 Nanocrystals within a Polyvinyl Butyral Laminate

Nicholas I. Cool, Carlos A. Larriuz, Randall James, Jaime R. Ayala, Anita, Mohammed Al-Hashimi, and Sarbajit Banerjee*

Cite This: *ACS Eng. Au* 2022, 2, 477–485

Read Online

ACCESS | Metrics & More | Article Recommendations | Supporting Information

ABSTRACT: The energy required to heat, cool, and illuminate buildings continues to increase with growing urbanization, engendering a substantial global carbon footprint for the built environment. Passive modulation of the solar heat gain of buildings through the design of spectrally selective thermochromic fenestration elements holds promise for substantially alleviating energy consumed for climate control and lighting. The binary vanadium(IV) oxide VO_2 manifests a robust metal—insulator transition that brings about a pronounced modulation of its near-infrared transmittance in response to thermal activation. As such, VO_2 nanocrystals are potentially useful as the active elements of transparent thermochromic films and coatings. Practical applications in retrofitting existing buildings requires the design of workflows to embed thermochromic fillers within industrially viable resins. Here, we describe the dispersion of VO_2 nanocrystals within a polyvinyl butyral laminate commonly used in the laminated glass industry as a result of its high optical clarity, toughness, ductility, and strong adhesion to glass. To form high-optical-clarity nanocomposite films, VO_2 nanocrystals are encased in a silica shell and functionalized with 3-methacryloxypropyltrimethoxysilane, enabling excellent dispersion of the nanocrystals in PVB through the formation of siloxane linkages and miscibility of the methacrylate group with the random copolymer. Encapsulation, functionalization, and dispersion of the core—shell VO_2@SiO_2 nanocrystals mitigates both Mie scattering and light scattering from refractive index discontinuities. The nanocomposite laminates exhibit a 22.3% modulation of NIR transmittance with the functionalizing moiety engendering a 77% increase of visible light transmittance as compared to unfunctionalized core—shell particles. The functionalization scheme and workflow demonstrated, here, illustrates a viable approach for integrating thermochromic functionality within laminated glass used for retrofitting buildings.

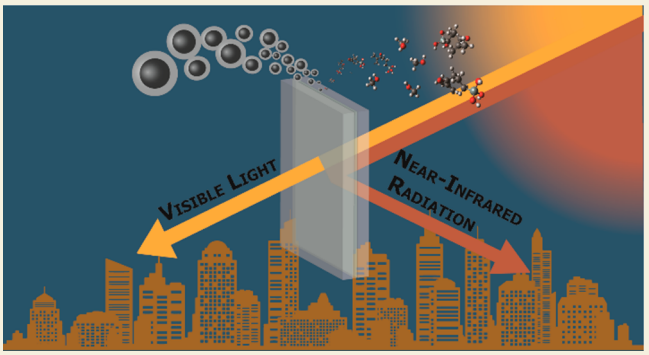

KEYWORDS: *thermochromic, metal—insulator transition, energy, optical properties, nanocomposite, thin film*

INTRODUCTION

The built environment is a large contributor to greenhouse gas emissions, both in terms of the embodied carbon footprint of construction materials and the operational energy consumption of buildings; the latter derives in large measure from interior climate control needs, such as heating, cooling, and lighting.[1−6] Fenestration elements, such as skylights, windows, and glass doors, are a key part of the building envelope and play a pivotal role in governing solar heat gain and heat loss to the external environment.[7,8] There has been much recent interest in the design of spectrally selective dynamically switchable fenestration elements to modulate diurnal and seasonal solar heat gain to improve the energy efficiency of buildings.[7−10] Conventionally, electrochromic materials have been studied for their potential to selectively modulate infrared transmittance; however, the cost involved in retrofitting existing structures have stymied their widespread adoption.[11−13] In contrast, thermochromic materials are passive systems wherein modulation of transmittance across a specific region of the electromagnetic spectrum is induced by thermally activating a phase transition or a structural transformation.[14,15] The onset temperature of thermochromic films can be modulated by site-selective modification of the active thermochromic elements, thereby enabling customization to the needs of specific climate zones.[16−18] Such passive films can

Received: June 18, 2022
Revised: July 15, 2022
Accepted: July 18, 2022
Published: July 21, 2022

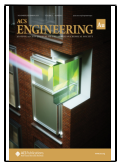

be directly adapted for retrofitting of fenestration elements. To facilitate compatibility with existing glass lamination processes, we report here the dispersion and embedding of active thermochromic fillers within a common laminate, polyvinyl butyral (PVB), which is widely used in automotive glass and solar cell module applications as a result of its high optical clarity, toughness, ductility, and excellent adhesion to glass.[19] The resulting thermochromic fenestration elements demonstrate selective modulation of infrared transmittance, as well as a high degree of visible light transmittance.

Nanocrystals of the binary transition metal oxide VO_2 are used as the active thermochromic filler.[7,8,14,20,21] VO_2 has a bandgap of 0.7 eV at low temperatures and undergoes a metal—insulator transition (MIT) that closes this bandgap at high temperatures, thus suppressing transmittance across the near- and mid-infrared regions of the electromagnetic spectrum. The electronic transition is accompanied, and arguably coupled, to a structural phase transition.[18,22,23] Recent first-principles calculations suggest that the transition from the rutile to M1 monoclinic phase, the latter being characterized by V−V dimerization in VO_2, is a Peierls-type transition but is governed by Mott physics in the presence of intersite exchange; thermally driven metallization is found to be exquisitely sensitive to the electronic temperature within this material.[18,24]

As a result of stresses accumulated upon repeated structural phase transformations, which are further exacerbated by substrate coupling, continuous films of VO_2 are prone to cracking and fatigue. An alternative strategy has focused on embedding ultrasmall nanocrystals of VO_2 within flexible polymer matrices, which enables facile accommodation of volume changes across phase transformations.[25] Utilizing the thermally triggered metallization of VO_2 nanocrystals in thermochromic fenestration elements requires not just control of particle composition and crystallinity (which govern the onset transition temperature, hysteresis, and sharpness) but also the particle dimensions, dispersion, interphase with the polymer matrix, and particle loading to alleviate common degradation mechanisms and mitigate light scattering.[7,8,10,16,18,25] Selection of the polymer matrix and functionalization of active fillers are both of critical importance to the design of high-optical-quality thermochromic fenestration elements. Films comprising large particles or agglomerations of smaller particles are prone to Mie scattering, which is a primary origin of optical haze.[10,25] In addition, the sharply discontinuous refractive index mismatch between VO_2 nanocrystals (2.0—2.8) and most typical polymer matrices (1.48—1.53) engenders light scattering at interfaces.[25−29] As such, considerable research has focused on encapsulation and surface functionalization of VO_2 nanocrystals to obtain smoother refractive index gradients, effective dispersion in the polymer matrix, and facile processability within laminate matrices.[30,31]

A prime laminate candidate for thermochromic fenestration applications is PVB, a thermoplastic that affords an optimal combination of high optical clarity and excellent thermochemical stability.[32,33] PVB is widely used in laminated glass and photovoltaic thin film modules.[34,35] Embedding VO_2 nanocrystals within PVB is particularly desirable for compatibility with current manufacturing processes. As-prepared VO_2 nanocrystals obtained from hydrothermal methods have a high density of surface hydroxyl groups, which renders them hydrophilic and poorly wetting to nonpolar polymers.[36,37] Since an intermediate refractive index material is necessary to mitigate the refractive index mismatch between VO_2 (2.0—2.8 depending on the phase and wavelength) and PVB (1.48), VO_2 nanocrystals are often encapsulated within a SiO_2 shell (refractive index of 1.8).[10,27,29,31,38,39] The SiO_2 shell further imbues protection from sintering and provides a handle for chemical functionalization based on the tethering of organofunctional silanes.[10,16,40] An important imperative is thus to design appropriate functionalization schemes to enable the dispersion and embedding of VO_2@SiO_2 nanocrystals in PVB. We report, here, the use of a coupling agent that is tethered to the SiO_2 shells encapsulating VO_2 nanocrystals and forms siloxane linkages with the PVB matrix. The resulting nanocomposite fenestration elements have been evaluated with respect to visible light transmittance, near-infrared (NIR) modulation, and overall modulation of the solar spectrum in addition to rheological considerations necessary for film fabrication by tape casting such as to ensure compatibility with retrofitting applications.

EXPERIMENTAL METHODS

Encapsulation of VO_2 Nanocrystals with a SiO_2 Shell and Surface Functionalization of VO_2@SiO_2 Core—Shell Nanoparticles

VO_2 nanocrystals with dimensions of 26 ± 8 nm, crystallized in the monoclinic phase, were prepared by Dimien, Inc., using a hydrothermal process.[41] In a typical method to constitute SiO_2 shells, 0.0726 g of VO_2 nanocrystals were dispersed in 128 mL of ethanol and 32 mL of DI water (ρ = 18.2 MΩ·cm, Barnstead International NANOpure Diamond system) by ultrasonication (Branson 5510) for 1 h. Ammonium hydroxide (1600 μL) and tetraethyl orthosilicate (300 μL) were added to the dispersion and allowed to stir at 25 °C for 24 h.[10,16] On the basis of our previous work, the selected concentration of tetraethyl orthosilicate and reaction time of 24 h yields a shell thickness of 19 ± 1 nm (vide infra).[16] Residual unreacted tetraethyl orthosilicate was removed from solution by centrifugation (8500 rpm, 10 min) (Heraeus Megafuge 8), followed by three washes with ethanol and one with acetone. The encapsulated nanocrystals were then dried under a flow of nitrogen on a Schlenk line at room temperature prior to functionalization with 3-methacryloxypropyltrimethoxysilane. This sequence of steps prevents the condensation and homogeneous nucleation of SiO_2 particles and ensures that SiO_2 deposition results in conformal coating of the surfaces of the VO_2 nanocrystals.

3-Methacryloxypropyltrimethoxysilane (KH570) (Sigma-Aldrich) (0.1091 g) was prepared by hydrolyzing the trimethoxysilane to form 3-methacryloxypropyltrihydoxysilane by treating it with 2 mL of a 4:1 (v/v) ethanol/water mixture. The pH of the solution was adjusted to 4 by the addition of glacial acetic acid and then ultrasonicated (Branson 5510) for 1 h. VO_2@SiO_2 core—shell nanoparticles (8 mg) were next dispersed into the 3-methacryloxypropyltrihydroxysilane solution by ultrasonicating for 1 h and then stirred for 18 h at 25 °C.

Dispersion of Functionalized VO_2@SiO_2 Nanoparticles in PVB and Casting of Nanocomposite Thin Films

VO_2@SiO_2-3-methacryloxypropyltrihydoxysilane was dispersed into a PVB dispersion by first heating 2.6166 g of PVB (Millipore Sigma) (MW 40 000−70 000) in 10 mL of ethanol under magnetic stirring until the polymer dispersion turned clear. Two modes of dispersing VO_2@SiO_2 nanoparticles in PVB were explored, extended magnetic stirring and shear mixing. In the first approach, functionalized VO_2@SiO_2-3-methacryloxypropyltrihydoxysilane nanoparticles were added to the PVB dispersion, which was allowed to stir for 18 h at 25 °C. In the second shear mixing approach, a FlackTek SpeedMixer (DAC 330−100 Pro) was used to disperse the nanoparticles by adding the PVB and VO_2@SiO_2-3-methacryloxypropyltrihydoxysilane nanoparticles into the mixer for 5 min at 3500 rpm.

https://doi.org/10.1021/acsengineeringau.2c00027
ACS Eng. Au 2022, 2, 477−485

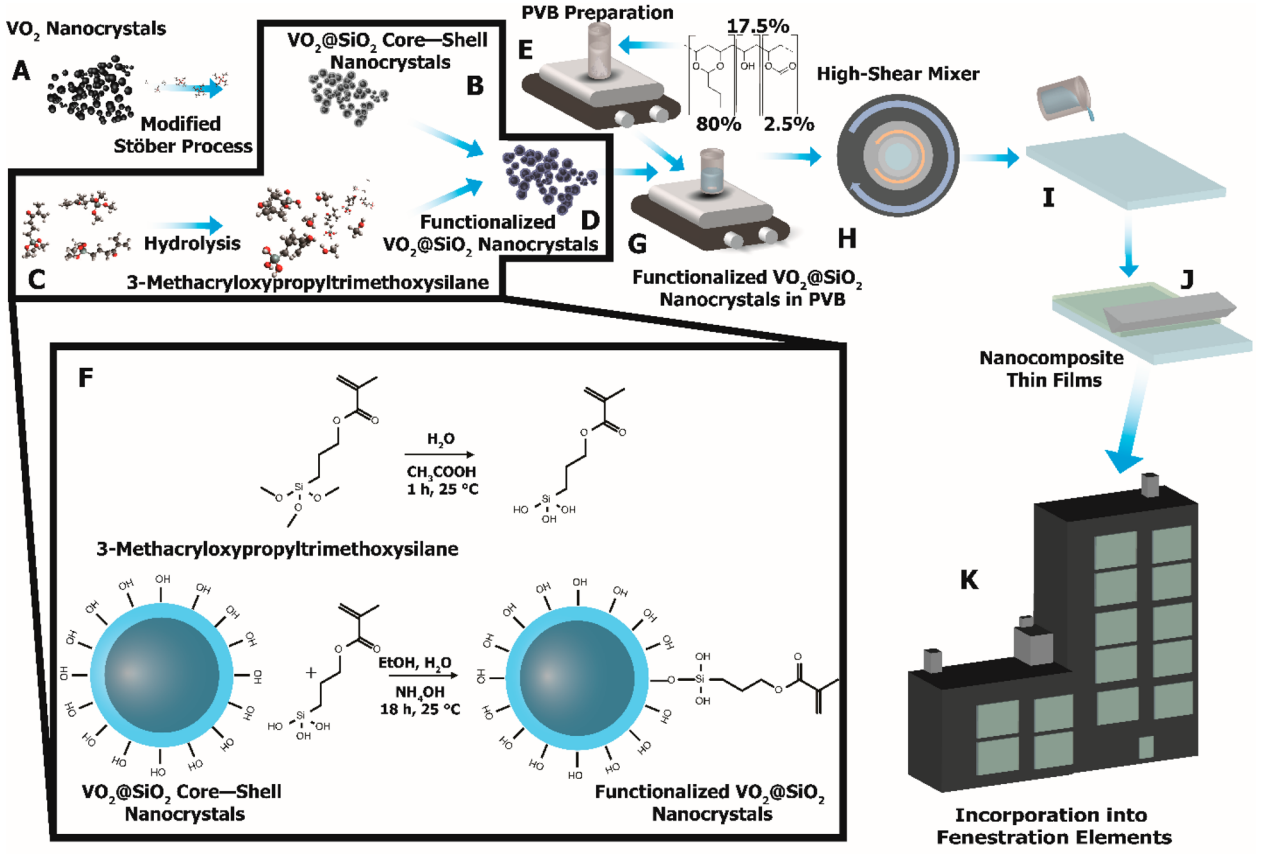

Figure 1. Schematic illustration of workflow for fabrication of thermochromic fenestration elements. The workflow illustrates (A, B) the encapsulation of VO_2 nanocrystals in a SiO_2 shell, (C, D, F) functionalization of the silica shell with 3-methacryloxypropyltrimethoxysilane, and (E−H) dispersion of the functionalized VO_2@SiO_2 nanoparticles within a PVB dispersion. The PVB dispersion is (I, J) tape casted as a wet film to form nanocomposite thin films on glass for fenestration applications.

Nanocomposite thin films were tape cast from the functionalized-VO_2@SiO_2 nanoparticle/PVB formulations onto 2.5 cm × 7.5 cm × 1.2 mm borosilicate glass microscope slides (VWR). The slides were first cleaned with ethanol and acetone, followed by preheating of the glass with a heat gun (Seekone SDL-2816). The PVB dispersion with VO_2@SiO_2 nanoparticles was then cast onto the glass slides at 65 °C using wet-film tape casting (BYK) at a thickness of 1 mm, followed by directed heating using a heat gun to remove any bubbles and ensure even drying of the films.[10]

Characterization and Evaluation of Thermochromic Performance

The VO_2@SiO_2 particles were analyzed using a Bruker Vertex 70 FT-IR spectrometer equipped with a Pike Technologies MIRacle with a diamond single reflection plate while using a globar (SiC) lamp as a mid-infrared source, with and without the addition of the 3-methacryloxypropyltrimethoxysilane. Upon dispersion into PVB, the optical properties of the films were determined through the use of a Bruker Vertex 70 FT-IR spectrometer using a globar (SiC) and tungsten source for the MIR and NIR, respectively. Optical transmittance spectra were acquired in transmission mode at 25 and 85 °C using a Pike Technologies heated solid transmission accessory. Optical microscopy was performed on the prepared films with and without a dispersing agent using an Olympus BX41 microscope with a LMPlanFLN 20× objective and a Euromex Iluminator EK-1 light source.

Values of ΔT_x were calculated using eqs 1 and 2:

$$T_x = \frac{\int \varphi_x(\lambda) T(\lambda) d\lambda}{\int \varphi_x(\lambda) d\lambda} \text{ where } x = \text{sol/lum/NIR} \quad (1)$$

$$\Delta T_x = T_x(\text{low temp}) - T_x(\text{high temp}) \quad (2)$$

where $\varphi_x(\lambda)$ is the solar irradiance spectrum for air mass 1.5 at a 37° global tilt and $T(\lambda)$ is the transmittance through the film at a specific wavelength. The values were computed before and after heating in the wavelength ranges 450—2500 nm (Sol), 450—750 nm (Lum), and 750—2500 nm (NIR), respectively.[42,43]

Powder X-ray diffraction (XRD) was performed using a Bruker D8-Focus Bragg−Brentano X-ray Powder Diffractometer with a Lynxeye PSD detector and a copper Kα source (λ = 1.5418 Å) for each sample.

Nanocrystals were cast onto an FCF-300-Cu grid by first dispersing the nanocrystals in acetone and then drop casting them onto the Cu grid. Transmission electron microscopy (TEM) was performed using a JEOL 2010 at an operating voltage of 200 kV and a beam current of 100 mA. The average particle size was then determined through ImageJ analysis software.

Differential scanning calorimetry was performed using a TA Instruments Q2000 instrument with a Tzero pan (901683.901) and Tzero lid (901671.901). The temperature was increased from −20 to 100 °C at a rate of 15 °C/min where it was held isothermally for 1 min the temperature was then lowered from 100 °C to −20 °C at a rate of 15 °C/min at which point the cycle was repeated three times.

Viscosity measurements were performed using a HR-2 Discovery hybrid rheometer with a parallel plate size of 8 mm, a trim gap of 320 μm, and a geometry gap of 300 μm. Data was collected at 25 and 65 °C for each formulation.

Infrared videos were taken of the films undergoing a MIT using an infrared-enabled iPhone camera with an 850 nm long-pass filter. This combination allows for sensitivity up to 1000 nm due to limitations of

https://doi.org/10.1021/acsengineeringau.2c00027
ACS Eng. Au 2022, 2, 477−485

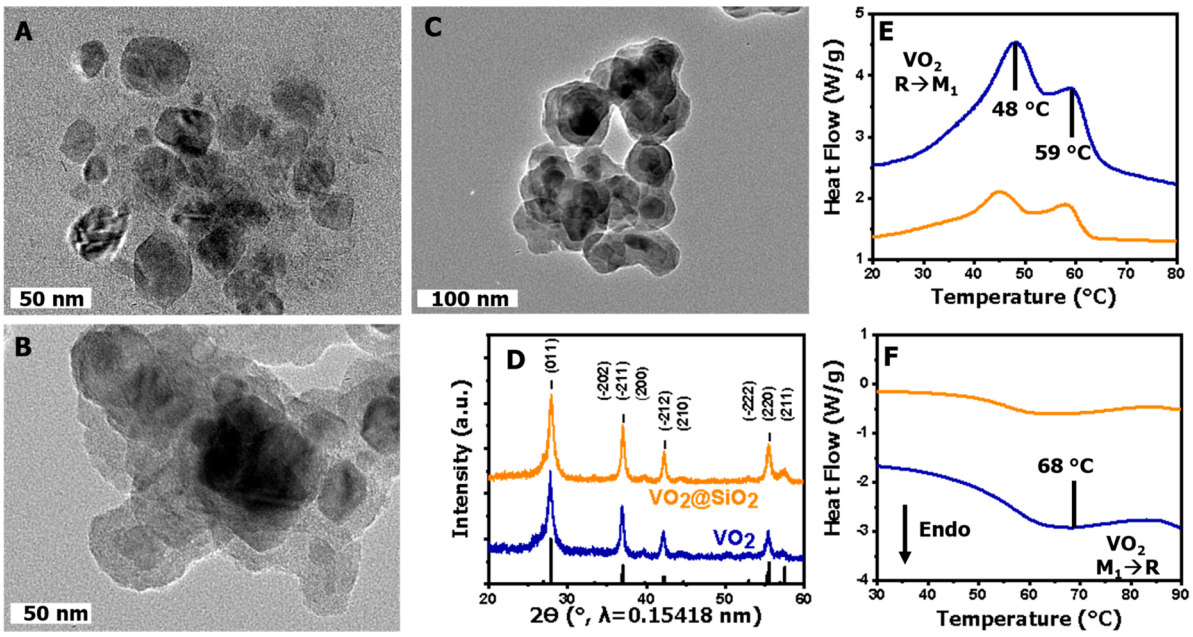

Figure 2. TEM images of VO_2 nanocrystals (A) without and (B, C) with a functionalized silica shell. (D) XRD patterns of VO_2 nanocrystals with (orange) and without (blue) a functionalized silica shell indexed to PDF 44-0252 corresponding to monoclinic VO_2. DSC traces of (E) the cooling transition and (F) the heating transition for VO_2 nanocrystals with (orange) and without (blue) a functionalized silica shell.

the complementary metal oxide semiconductor (CMOS) sensor of the camera.

RESULTS AND DISCUSSION

PVB is generally regarded to be a random copolymer comprising vinyl alcohol and vinyl butyral units.[44] Commercial PVB (Butvar B-98) comprises ~80% poly(vinyl butyral), 10—20% poly(vinyl alcohol), and 2.5% poly(vinyl acetate). Figure 1 illustrates the workflow used to disperse VO_2 nanocrystals within the PVB matrix, and for the preparation of nanocomposite fenestration elements. Hydrothermally prepared quasi-spherical VO_2 nanocrystals (26 ± 8 nm in diameter) crystallized in the M1 phase are encapsulated within ~19 ± 1 nm thick amorphous SiO_2 shells (Figure 2). The M1 structure of the nanocrystals is retained upon SiO_2 encapsulation. DSC thermograms (Figure 2E and F) show well-defined endothermic and two separate exothermic features corresponding to lattice enthalpy and conduction entropy changes across M1 → R and R → M1 transitions, respectively. The symmetry-raising M1 → R transition is readily nucleated at twin planes between monoclinic variants and is not generally nucleation limited.[22] The two separate features observed for the R → M1 transition reflects the nucleation limitations common to smaller particles. The R → M1 transition is nucleated at point defects such as oxygen vacancies; the concentration of these defects is greatly decreased at nanometer-sized dimensions as a result of the proclivity of the defects to migrate to surfaces where they are healed. The distinctive exothermic features correspond to variations in defect density within the ultrasmall VO_2 nanocrystals.[16,22,25,45]

Ultrasmall dimensions of active fillers, below the wavelength of visible light, are a necessary but not sufficient criterion for mitigating light scattering in thermochromic fenestration elements.[10,25] Agglomerated ultrasmall particles can scatter light much the same way as larger particles, and thus, a key imperative is to ensure the effective dispersion of the particles within laminate matrices.[25] Encapsulation within an amorphous SiO_2 shell renders the surfaces of the core—shell VO_2@SiO_2 nanoparticles amenable to further functionalization by reaction with silanes. Specifically, 3-methacryloxypropyltrimethoxysilane has been used to facilitate the dispersion of VO_2@SiO_2 nanoparticles into PVB.[36,37,46] Figure 1F shows the sequence of reactions used to tether the silane to the surfaces of VO_2@SiO_2 nanoparticles through siloxane linkages. The pendant 3-methacryloxypropyl groups of the silane allow for dispersion and compatibilization of the VO_2@SiO_2 nanoparticles within PVB.[36,37,46] The grafting of 3-methacryloxypropyltrimethoxysilane onto the SiO_2 shells has been confirmed by FTIR spectroscopy (Figure 3). Bands corresponding to C−H stretches are observed at 2952 and 2883 cm^{-1}, respectively; −C═O bands are observed at 1718 cm^{-1}, and C═C stretches are observed at 1636 cm^{-1}.

The functionalized VO_2@SiO_2 nanoparticles have been blended with a 10—40 wt % PVB dispersion in ethanol. On the basis of the measured rheology of the blends and the optical clarity of the cast films, a 30 wt % PVB loading in ethanol is selected as the optimal polymer loading to prepare thermochromic formulations. Lower weight percent concentrations of PVB lead to nonuniform drying, resulting in "wrinkled" films, whereas the rheological characteristics of ~40 wt % PVB (13 210 cP at 25 °C) makes it difficult to cast optically clear thin films (Figure S1). For the 30 wt % PVB dispersion in ethanol, the viscosity is decreased from 5,914 cP at 25 °C to 814 cP at 65 °C, which allows for blade coating to be used to cast homogeneous thin films. The thermoplastic films are annealed using a heat gun to remove imperfections, such as voids. Figure S2 shows digital photographs of PVB films cast from different concentrations of PVB in ethanol.

The 30 wt % PVB in ethanol dispersion is blended with functionalized and bare VO_2@SiO_2 nanoparticles as sketched in Figure 1. The high viscosity of PVB presents a challenge to obtaining homogeneous dispersions. We first contrast the effects of the mode of mixing used to disperse functionalized VO_2@SiO_2 nanoparticles in PVB. Functionalized VO_2@SiO_2

https://doi.org/10.1021/acsengineeringau.2c00027
ACS Eng. Au 2022, 2, 477−485

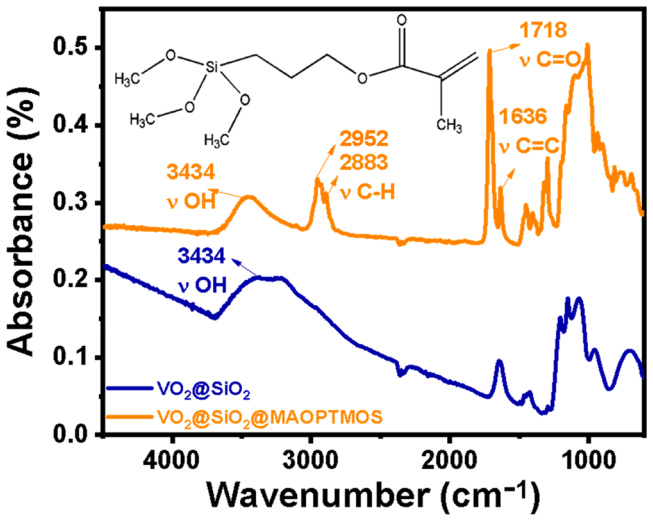

Figure 3. FTIR-ATR spectra of VO_2@SiO_2 with a loading of 6.1 wt % 3-methacryloxypropyltrihydoxysilane/VO_2@SiO_2 (orange) and without any additional functionalization (blue). Assignments of the most prominent IR modes are labeled. The inset shows the structure of 3-methacryloxypropyltrimethoxysilane prior to hydrolysis.

nanoparticles with 6.1 wt % of the pendant silane are blended into PVB at a loading of 0.8 mg/mL using magnetic stirring or high shear mixing. Extended magnetic stirring for 18 h is required to obtain well-dispersed formulations in the former approach. In contrast, shear mixing uses a dual asymmetric centrifugal mechanism to rapidly spin the container at 3500 rpm in opposite directions, which yields homogeneous compounded dispersions within 5 min. The compounded dispersions have a viscosity of 814 cP and have been used to cast nanocomposite films using wet-film tape casting as described in the Experimental Methods section. Visible—NIR transmittance spectra are used to interrogate the thermochromic performance of the nanocomposite thin films tape cast from PVB blends.

Figure S3 plots visible—NIR transmittance spectra obtained well below and above the VO_2 metal—insulator transition temperature for nanocomposite films cast from VO_2@SiO_2 nanoparticles blended into PVB. A pronounced modulation of NIR transmittance is observed starting at ∼700 nm corresponding to the thermally driven closing of the bandgap of VO_2. The visible light transmittance is only marginally altered. Figure S3 shows a notable increase in the integrated NIR modulation from 19.3% to 22.3% for films cast from shear-mixed samples as compared to the magnetically stirred formulations. In addition, the films cast from shear-mixed samples show improved homogeneity in visible transmittance values.[25] In films cast from magnetically stirred blends, the visible light transmittance at 555 nm varies from 43.1—54.1%, whereas the films cast from shear mixed samples show a closer spread of 44.8—47.8%, indicating a much more homogeneous dispersion. On the basis of these results, shear mixing has been adopted as the method of dispersing VO_2@SiO_2 nanoparticles within PVB.

We next contrast the role of surface functionalization of VO_2@SiO_2 nanoparticles in mediating improved dispersion in PVB. The VO_2 nanocrystals are first encapsulated within SiO_2 shells to alleviate the mismatch in refractive index between VO_2 (2.0—2.8 depending on the phase, temperature, and wavelength of light) and the laminate PVB matrix (∼1.48). By encapsulating the VO_2 nanocrystals in a SiO_2 shell with an intermediate refractive index of ca. 1.8, light scattering at the discontinuous filler/laminate-matrix interface is greatly alleviated.[10,27,47−49] In the absence of a dispersing agent, hydrophilic VO_2@SiO_2 nanoparticles remain somewhat agglomerated even upon shear mixing, which gives rise to Mie scattering that degrades the optical clarity of the films.[25,50,51] The importance of the coupling agent is readily apparent in Figure 4A, where the use of surface functionalization suppresses haze and increases the visible light transmittance from ∼26.9% to 47.6%. Contrasting VO_2@SiO_2 nanocomposite fenestration elements with different extents of functionalization for the same overall active filler loading (0.8 mg/mL), functionalization with 6.1 wt % is found to be optimal, yielding NIR modulation of 22.3% and T_{555nm} of 47.6%. The decreased haze and increased visible transmittance is further evident in the digital photographs shown in Figure 5A, B, D, F, and H, wherein a ∼77% increase in transmittance is observed as a result of the reduction in haze by mitigating particle agglomeration through the use of surface functionalization. Optical microscopy images of functionalized and

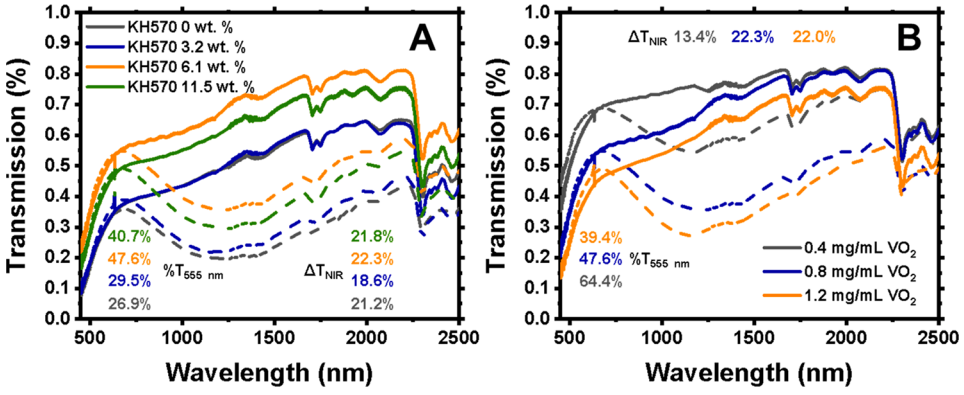

Figure 4. Examining the influence of surface functionalization and active filler loading. (A) Optical transmittance spectra of VO_2@SiO_2/PVB films prepared by shear mixing as a function of different concentrations of the dispersing agent. The loading of active filler is held constant at 0.8 mg/mL of VO_2@SiO_2 nanoparticles in PVB. The 25 °C spectra are plotted as solid lines, whereas the 85 °C spectra are plotted as dashed lines. The % T_{555nm} and ΔT_{NIR} denote the percentage transmittance at 555 nm and the integrated near-infrared modulation of the electromagnetic spectrum. (B) Optical transmittance spectra of VO_2@SiO_2/PVB films prepared by shear mixing as a function of different loadings of the active filler. The concentration of the dispersing agent is kept constant at 6.1 wt. %.

https://doi.org/10.1021/acsengineeringau.2c00027
ACS Eng. Au 2022, 2, 477−485

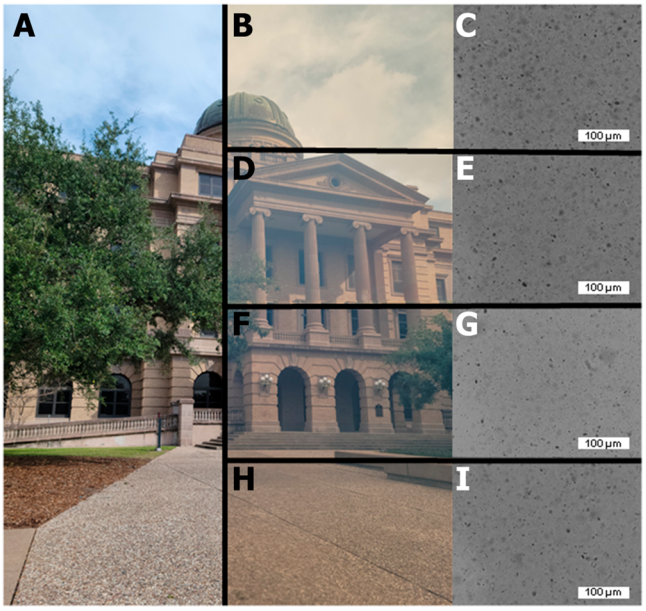

Figure 5. (A) Digital photographs without additional film. (B, D, F, H) Digital photographs taken through a film with a 3-methacryloxypropyltrimethoxysilane concentration of 0, 3.2, 6.1, and 11.5 wt. % respectively. (C, E, G, I) Optical microscopy image of films with a 3-methacryloxypropyltrimethoxysilane concentration of 0, 3.2, 6.1, and 11.5 wt. % respectively.

unfunctionalized VO_2@SiO_2 PVB nanocomposite films in Figures 5C, E, G, and I further corroborate the greater agglomeration of particles without silane functionalization.

Figure 4B contrasts visible—NIR transmittance spectra of shear-mixed VO_2@SiO_2 nanoparticles blended into PVB varying the active filler loading while holding the concentration of the dispersing agent constant at the optimal value of 6.1 wt %. An increase in integrated NIR modulation is observed with increased active filler loading (Figure 4B); however, the visible light transmittance is concomitantly decreased. An active filler loading of 0.8 mg/mL provides the optimal combination of NIR modulation and visible light transmittance. Consequently, considering the various factors examined here, a formulation with a VO_2@SiO_2 nanoparticle loading of ∼0.8 mg/mL, concentration of surface functionalizing silane at 6.1 wt %, blended with a 30 wt % PVB dispersion in ethanol show the optimal thermochromic properties. The resulting film exhibits $\%T_{555nm}$ of 47.6%, increasing to 52% at 600 nm, and a ΔT_{NIR} of 22.3% (Figure 5F). Video S1 shows the modulation of NIR transmittance measured between 850 and 1000 nm using an 850 nm long-pass filter and an infrared enabled camera. Even though the transmittance contrast is relatively low between 850—1000 nm (Figure 4), a clear modulation of NIR transmittance is observed. Table 1 contrasts the ΔT_{Sol}, ΔT_{NIR}, ΔT_{lum}, and % transmittance values for tape-cast films with varying active filler loadings and concentrations of the functionalizing agent.

The results show the critical importance of not just crystallite size and graded refractive index interfaces,[10,25,26] but also optimal particle dispersion to mitigate light scattering derived from agglomeration of active filers in a high-optical-clarity laminate matrix. Surface functionalization of VO_2@SiO_2 nanoparticles with 3-methacryloxypropyltrihydoxysilane allows for formation of siloxane linkages with reactive hydroxyl groups in PVB, as shown in Figure 1. PVB can further interact with methacrylate functional groups present on 3-methacryloxypropyltrihydoxysilane, thereby providing an additional means of engendering miscibility. While PVB and PMMA are generally immiscible, repulsive interactions between vinyl alcohols and vinyl butyral units within PVB chains are alleviated through interactions with methacrylate groups, providing a reasonable interaction parameter value for smaller methacrylate fragments and higher vinyl alcohol concentrations.[44] Such segmental interactions are particularly important when attempting to control the miscibility of a copolymer and homopolymer system. The conformations of copolymer systems, such as in PVB, are governed by repulsive forces between the vinyl alcohol (VA), vinyl butyral (VB), and vinyl acetate (VAc) segments. The segmental interactions in the PVB copolymer are dominated by the former two majority components. The VA segments are hydrophilic, whereas the VB segments are hydrophobic in nature, which leads to repulsive interactions between the segments. The repulsive interactions between VA and VB segments are somewhat alleviated through the inclusion of additional homopolymer segments such as the pendant methacrylate moieties grafted onto the surface of VO_2@SiO_2 particles. Methacrylate interactions mediating VA/VB segmental repulsions in PVB provides a means of engendering miscibility and enhances the dispersion of the 3-methacryloxypropyltrimethoxysilane-functionalized VO_2@SiO_2 nanocrystals.[44] The formation of siloxane linkages and favorable segmental interactions facilitate dispersion of the functionalized VO_2@SiO_2 nanocrystals in PVB, which in turn substantially alleviates Mie scattering mechanisms.

CONCLUSIONS

We present, here, an approach to embed VO_2 nanocrystal thermochromic fillers within a high optical clarity PVB resin that is commonly used in laminated glass and photovoltaic thin film modules. The active thermochromic fillers prepared with nanometer-sized dimensions to mitigate Mie scattering are encapsulated within a SiO_2 matrix to obtain a continuous gradation of refractive indices and to provide a handle for further functionalization. Surface functionalization of VO_2@SiO_2 core—shell nanoparticles with 3-methacryloxypropyltrimethoxysilane enables improved dispersion of the thermo-

Table 1. ΔT_{Sol}, ΔT_{NIR}, ΔT_{lum}, % Transmittance Values for Tape-Cast Films with Varying 3-Methacryloxypropyltrimethoxysilane Concentrations at a Constant Loading of 0.8 mg/mL and Varying Loading Concentrations at a Constant 3-Methacryloxypropyltrimethoxysilane Concentration of 6.1 wt. %

	3-methacryloxypropyltrimethoxysilane concentration				nanocrystal loading		
	0 wt %	3.2 wt %	6.1 wt %	11.5 wt %	0.4 mg/mL	0.8 mg/mL	1.2 mg/mL
ΔT_{Sol}	10.8%	8.5%	10.7%	10.4%	5.1%	10.7%	9.5%
ΔT_{NIR}	21.2%	18.6%	22.3%	21.8%	13.4%	22.3%	22.0%
ΔT_{lum}	1.2%	−0.8%	0.8%	−0.1%	−2.4%	0.8%	−2.0%

https://doi.org/10.1021/acsengineeringau.2c00027
ACS Eng. Au 2022, 2, 477−485

chromic fillers within PVB thin films as a result of the formation of siloxane linkages with remnant vinyl alcohol groups and the miscibility of pendant methacrylate moieties with the random copolymer of vinyl alcohol and vinyl butyral units. By mitigating agglomeration and facilitating dispersion of the particles within the host matrix, Mie scattering mechanisms are substantially alleviated. Optimal formulations show a transmittance of 47.6% at 555 nm, as well as NIR modulation of 22.3%, rivaling previously reported thermochromic VO_2 films.[10,16,25] Future work will focus on incorporating additional gradation of refractive indices, such as through incorporation of multiple shells of intermediate refractive index (GeO_2, Al_2O_3), to further enhance clarity and improve resistance to oxidation, as well as the characterization and enhancement of the durability of the nanocomposite films.

■ ASSOCIATED CONTENT

Supporting Information

The Supporting Information is available free of charge at https://pubs.acs.org/doi/10.1021/acsengineeringau.2c00027.

Viscosity vs temperature profile of PVB formulations; digital photographs of PVB films; and optical transmittance spectra of films prepared by shear mixing vs stirring (PDF)

Infrared time-lapse video of thermochromic transition (AVI)

■ AUTHOR INFORMATION

Corresponding Author

Sarbajit Banerjee − *Department of Chemistry, Texas A&M University, College Station, Texas 77843-3012, United States; Department of Materials Science and Engineering, Texas A&M University, College Station, Texas 77843-3012, United States;* orcid.org/0000-0002-2028-4675; Email: banerjee@chem.tamu.edu

Authors

Nicholas I. Cool − *Department of Chemistry, Texas A&M University, College Station, Texas 77843-3012, United States; Department of Materials Science and Engineering, Texas A&M University, College Station, Texas 77843-3012, United States*

Carlos A. Larriuz − *Department of Chemistry, Texas A&M University, College Station, Texas 77843-3012, United States; Department of Chemistry, University of Puerto Rico, Cayey, Puerto Rico 00736, United States*

Randall James − *Department of Chemistry, Texas A&M University, College Station, Texas 77843-3012, United States*

Jaime R. Ayala − *Department of Chemistry, Texas A&M University, College Station, Texas 77843-3012, United States; Department of Materials Science and Engineering, Texas A&M University, College Station, Texas 77843-3012, United States*

Anita − *Department of Chemistry, Texas A&M University, College Station, Texas 77843-3012, United States; Department of Materials Science and Engineering, Texas A&M University, College Station, Texas 77843-3012, United States*

Mohammed Al-Hashimi − *Department of Chemistry, Texas A&M University at Qatar, Doha 23874, Qatar;* orcid.org/0000-0001-6015-2178

Complete contact information is available at: https://pubs.acs.org/10.1021/acsengineeringau.2c00027

Author Contributions

CRediT: **Nicholas I. Cool** conceptualization (lead), data curation (lead), investigation (lead), visualization (lead), writing-original draft (lead); **Carlos A Larriuz** formal analysis (supporting), investigation (supporting), methodology (supporting); **Randall James** data curation (supporting), formal analysis (supporting), investigation (supporting); **Jaime R Ayala** investigation (supporting), methodology (supporting); **Anita** formal analysis (supporting), investigation (supporting), methodology (supporting); **Mohammed Al-Hashimi** project administration (supporting), supervision (supporting), writing-review & editing (supporting); **Sarbajit Banerjee** conceptualization (equal), project administration (lead), supervision (lead), writing-review & editing (lead).

Notes

The authors declare no competing financial interest.

■ ACKNOWLEDGMENTS

This project was initially funded by Vanitec. N.I.C. acknowledges the support of the NSF under a Graduate Research Fellowship Grant DGE:1746932. We gratefully acknowledge financial support from the Qatar National Research Fund, Project Number NPRP11S-1204-170062. J.R.A. acknowledges support from a Department of Energy IBUILD Fellowship.

■ REFERENCES

(1) Omer, A. M. Energy, Environment and Sustainable Development. *Renewable and Sustainable Energy Reviews* **2008**, *12* (9), 2265−2300.

(2) Kobeyev, S.; Tokbolat, S.; Durdyev, S. Design and Energy Performance Analysis of a Hotel Building in a Hot and Dry Climate: A Case Study. *Energies* **2021**, *14* (17), 5502.

(3) Granqvist, C. G. Transparent Conductors as Solar Energy Materials: A Panoramic Review. *Sol. Energy Mater. Sol. Cells* **2007**, *91* (17), 1529−1598.

(4) Dixit, M. K.; Culp, C. H.; Fernandez-Solis, J. L. Embodied Energy of Construction Materials: Integrating Human and Capital Energy into an IO-Based Hybrid Model. *Environ. Sci. Technol.* **2015**, *49* (3), 1936−1945.

(5) Akbarnezhad, A.; Xiao, J. Estimation and Minimization of Embodied Carbon of Buildings: A Review. *Buildings* **2017**, *7* (1), 5.

(6) Bajpayee, A.; Farahbakhsh, M.; Zakira, U.; Pandey, A.; Ennab, L. A.; Rybkowski, Z.; Dixit, M. K.; Schwab, P. A.; Kalantar, N.; Birgisson, B.; Banerjee, S. In situ Resource Utilization and Reconfiguration of Soils Into Construction Materials for the Additive Manufacturing of Buildings. *Frontiers in Materials* **2020**, *7*, 52.

(7) Cao, X.; Chang, T.; Shao, Z.; Xu, F.; Luo, H.; Jin, P. Challenges and Opportunities toward Real Application of VO_2-Based Smart Glazing. *Matter* **2020**, *2* (4), 862−881.

(8) Cui, Y.; Ke, Y.; Liu, C.; Chen, Z.; Wang, N.; Zhang, L.; Zhou, Y.; Wang, S.; Gao, Y.; Long, Y. Thermochromic VO_2 for Energy-Efficient Smart Windows. *Joule* **2018**, *2* (9), 1707−1746.

(9) Wang, Y.; Runnerstrom, E. L.; Milliron, D. J. Switchable Materials for Smart Windows. *Annu. Rev. Chem. Biomol. Eng.* **2016**, *7*, 283−304.

(10) Fleer, N. A.; Pelcher, K. E.; Zou, J.; Nieto, K.; Douglas, L. D.; Sellers, D. G.; Banerjee, S. Hybrid Nanocomposite Films Comprising Dispersed VO_2 Nanocrystals: A Scalable Aqueous-Phase Route to Thermochromic Fenestration. *ACS Appl. Mater. Interfaces* **2017**, *9* (44), 38887−38900.

(11) Chernova, N. A.; Roppolo, M.; Dillon, A. C.; Whittingham, M. S. Layered Vanadium and Molybdenum Oxides: Batteries and Electrochromics. *J. Mater. Chem.* **2009**, *19* (17), 2526−2552.
(12) Wu, W.; Wang, M.; Ma, J.; Cao, Y.; Deng, Y. Electrochromic Metal Oxides: Recent Progress and Prospect. *Adv. Electron. Mater.* **2018**, *4* (8), 1800185.
(13) Granqvist, C. G.; Arvizu, M. A.; Bayrak Pehlivan, İ.; Qu, H. Y.; Wen, R. T.; Niklasson, G. A. Electrochromic Materials and Devices for Energy Efficiency and Human Comfort in Buildings: A Critical Review. *Electrochim. Acta* **2018**, *259*, 1170−1182.
(14) Andrews, J. L.; Santos, D. A.; Meyyappan, M.; Williams, R. S.; Banerjee, S. Building Brain-Inspired Logic Circuits from Dynamically Switchable Transition-Metal Oxides. *Trends in Chemistry* **2019**, *1* (8), 711−726.
(15) Zhang, W.; Ji, X.; Peng, B.-J.; Che, S.; Ge, F.; Liu, W.; Al-Hashimi, M.; Wang, C.; Fang, L. High-Performance Thermoresponsive Dual-Output Dye System for Smart Textile Application. *Adv. Funct. Mater.* **2020**, *30* (3), 1906463.
(16) Cool, N. I.; Sellers, D. G.; Al-Hashimi, M.; Banerjee, S. Near-Ambient Nanocomposite Thermochromic Fenestration Elements from Post-Encapsulation-Annealed Tungsten-Alloyed Vanadium(IV) Oxide Nanocrystals. *ACS Appl. Energy Mater.* **2022**, *5* (4), 4829−4839.
(17) Sellers, D. G.; Braham, E. J.; Villarreal, R.; Zhang, B.; Parija, A.; Brown, T. D.; Alivio, T. E. G.; Clarke, H.; De Jesus, L. R.; Zuin, L.; Prendergast, D.; Qian, X.; Arroyave, R.; Shamberger, P. J.; Banerjee, S. Atomic Hourglass and Thermometer Based on Diffusion of a Mobile Dopant in VO_2. *J. Am. Chem. Soc.* **2020**, *142* (36), 15513−15526.
(18) Schofield, P.; Braham, E. J.; Zhang, B.; Andrews, J. L.; Drozdick, H. K.; Zhao, D.; Zaheer, W.; Gurrola, R. M.; Xie, K.; Shamberger, P. J.; Qian, X.; Banerjee, S. Decoupling the Metal-Insulator Transition Temperature and Hysteresis of VO_2 using Ge Alloying and Oxygen Vacancies. *Chem. Commun.* **2022**, *58* (46), 6586−6589.
(19) Zhang, X.; Hao, H.; Shi, Y.; Cui, J. The Mechanical Properties of Polyvinyl Butyral (PVB) at High Strain Rates. *Construction and Building Materials* **2015**, *93*, 404−415.
(20) Gao, Y.; Luo, H.; Zhang, Z.; Kang, L.; Chen, Z.; Du, J.; Kanehira, M.; Cao, C. Nanoceramic VO_2 Thermochromic Smart Glass: A Review on Progress in Solution Processing. *Nano Energy* **2012**, *1* (2), 221−246.
(21) Wang, S.; Jiang, T.; Meng, Y.; Yang, R.; Tan, G.; Long, Y. Scalable Thermochromic Smart Windows with Passive Radiative Cooling Regulation. *Science* **2021**, *374* (6574), 1501−1504.
(22) Braham, E. J.; Sellers, D.; Emmons, E.; Villarreal, R.; Asayesh-Ardakani, H.; Fleer, N. A.; Farley, K. E.; Shahbazian-Yassar, R.; Arròyave, R.; Shamberger, P. J.; Banerjee, S. Modulating the Hysteresis of an Electronic Transition: Launching Alternative Transformation Pathways in the Metal-Insulator Transition of Vanadium(IV) Oxide. *Chem. Mater.* **2018**, *30* (1), 214−224.
(23) Whittaker, L.; Patridge, C. J.; Banerjee, S. Microscopic and Nanoscale Perspective of the Metal-Insulator Phase Transitions of VO_2: Some New Twists to an Old Tale. *J. Phys. Chem. Lett.* **2011**, *2* (7), 745−758.
(24) Brito, W. H.; Aguiar, M. C. O.; Haule, K.; Kotliar, G. Metal-Insulator Transition in VO_2: A DFT + DMFT Perspective. *Phys. Rev. Lett.* **2016**, *117* (5), 056402.
(25) Fleer, N. A.; Pelcher, K. E.; Nieto, K.; Braham, E. J.; Zou, J.; Horrocks, G. A.; Naoi, Y.; Depner, S. W.; Schultz, B. J.; Amano, J.; Sellers, D. G.; Banerjee, S. Elucidating the Crystallite Size Dependence of the Thermochromic Properties of Nanocomposite VO_2 Thin Films. *ACS Omega* **2018**, *3* (10), 14280−14293.
(26) Naoi, Y.; Amano, J. Optimization of VO_2 Nanowire Polymer Composite Thermochromic Films by Optical Simulation. *J. Appl. Phys.* **2016**, *120* (23), 235301.
(27) Currie, M.; Mastro, M. A.; Wheeler, V. D. Characterizing the Tunable Refractive Index of Vanadium Dioxide. *Opt. Mater. Express* **2017**, *7* (5), 1697−1707.
(28) Horwitz, J. Infrared Refractive Endex of Oolyethylene and a Polyethylene-Based Material. *Optical Engineering* **2011**, *50* (9), 093603.
(29) El-Din, N. M. S.; Sabaa, M. W. Thermal Degradation of Poly(vinyl butyral) Laminated Safety Glass. *Polym. Degrad. Stab.* **1995**, *47* (2), 283−288.
(30) Zhao, L.; Miao, L.; Liu, C.; Li, C.; Asaka, T.; Kang, Y.; Iwamoto, Y.; Tanemura, S.; Gu, H.; Su, H. Solution-Processed VO_2-SiO_2 Composite Films with Simultaneously Enhanced Luminous Transmittance, Solar Modulation Ability and Anti-Oxidation property. *Sci. Rep.* **2015**, *4* (1), 7000.
(31) Wang, M.; Tian, J.; Zhang, H.; Shi, X.; Chen, Z.; Wang, Y.; Ji, A.; Gao, Y. Novel Synthesis of Pure VO_2@SiO_2 Core@Shell Nanoparticles to Improve the Optical and Anti-Oxidant Properties of a VO_2 Film. *RSC Adv.* **2016**, *6* (110), 108286−108289.
(32) Tang, H.; Su, Y.; Tan, J.; Hu, T.; Gong, J.; Xiao, L. Optical Properties and Thermal Stability of Poly(vinyl butyral) Films embedded with LaB_6@SiO_2 Core-Shell Nanoparticles. *Superlattices Microstruct.* **2014**, *75*, 908−915.
(33) Kumar, P.; Khan, N.; Kumar, D. Polyvinyl Butyral (PVB), Versetile Template for Desogning Nanocomposite/Composite Materials: A Review. *Green Chemistry & Technology Letters* **2016**, *2*, 185.
(34) Serafinavičius, T.; Lebet, J.-P.; Louter, C.; Lenkimas, T.; Kuranovas, A. Long-Term Laminated Glass Four Point Bending Test with PVB, EVA and SG Interlayers at Different Temperatures. *Procedia Engineering* **2013**, *57*, 996−1004.
(35) Chen, S.; Zang, M.; Wang, D.; Yoshimura, S.; Yamada, T. Numerical Analysis of Impact Failure of Automotive Laminated Glass: A Review. *Composites Part B: Engineering* **2017**, *122*, 47−60.
(36) Mallakpour, S.; Madani, M. The Effect of the Coupling Agents KH550 and KH570 on the Nanostructure and Interfacial Interaction of Zinc Oxide/Chiral Poly(amide-imide) Nanocomposites Containing L-Leucine Amino Acid Moieties. *J. Mater. Sci.* **2014**, *49* (14), 5112−5118.
(37) Ma, S.-r.; Shi, L.-y.; Feng, X.; Yu, W.-j.; Lu, B. Graft Modification of ZnO Nanoparticles with Silane Coupling Agent KH570 in mixed solvent. *Journal of Shanghai University (English Edition)* **2008**, *12* (3), 278−282.
(38) Gao, Y.; Wang, S.; Luo, H.; Dai, L.; Cao, C.; Liu, Y.; Chen, Z.; Kanehira, M. Enhanced Chemical Stability of VO_2 Nanoparticles by the Formation of SiO_2/VO_2 Core/Shell Structures and the Application to Transparent and Flexible VO_2-Based Composite Foils with Excellent Thermochromic Properties for Solar Heat Control. *Energy Environ. Sci.* **2012**, *5* (3), 6104−6110.
(39) Şahan, N.; Paksoy, H. Determining Influences of SiO_2 Encapsulation on Thermal Energy Storage Properties of Different Phase Change Materials. *Sol. Energy Mater. Sol. Cells* **2017**, *159*, 1−7.
(40) Zhou, X.; Meng, Y.; Vu, T. D.; Gu, D.; Jiang, Y.; Mu, Q.; Li, Y.; Yao, B.; Dong, Z.; Liu, Q.; Long, Y. A New Strategy of Nanocompositing Vanadium Dioxide with Excellent Durability. *Journal of Materials Chemistry A* **2021**, *9* (28), 15618−15628.
(41) Schultz, B. J.; Depner, S. W. Vanadium Oxide Compositions and Systems and Methods for Creating Them. US Patent 10889505B2, 2021.
(42) Liu, C.; Balin, I.; Magdassi, S.; Abdulhalim, I.; Long, Y. Vanadium Dioxide Nanogrid Films for High Transparency Smart Architectural Window Applications. *Opt. Express* **2015**, *23* (3), A124−A132.
(43) Li, S.-Y.; Niklasson, G. A.; Granqvist, C. G. Nanothermochromics with VO_2-Based Core-Shell Structures: Calculated Luminous and Solar Optical Properties. *J. Appl. Phys.* **2011**, *109* (11), 113515.
(44) Chen, W.; David, D. J.; MacKnight, W. J.; Karasz, F. E. Miscibility and Phase Behavior in Blends of Poly(vinyl butyral) and Poly(methyl methacrylate). *Macromolecules* **2001**, *34* (12), 4277−4284.
(45) Yano, A.; Clarke, H.; Sellers, D. G.; Braham, E. J.; Alivio, T. E. G.; Banerjee, S.; Shamberger, P. J. Toward High-Precision Control of

https://doi.org/10.1021/acsengineeringau.2c00027
ACS Eng. Au 2022, 2, 477−485

Transformation Characteristics in VO_2 through Dopant Modulation of Hysteresis. *J. Phys. Chem. C* **2020**, *124* (39), 21223−21231.
(46) Wang, Z.; Yuan, L.; Liang, G.; Gu, A. Mechanically Durable and Self-Healing Super-Hydrophobic Coating with Hierarchically Structured KH570 Modified SiO_2-Decorated Aligned Carbon Nanotube Bundles. *Chem. Eng. J.* **2021**, *408*, 127263.
(47) Hebert, K. J.; Zafar, S.; Irene, E. A.; Kuehn, R.; McCarthy, T. E.; Demirlioglu, E. K. Measurement of the Refractive Index of Thin SiO_2 Films using Tunneling Current Oscillations and Ellipsometry. *Appl. Phys. Lett.* **1996**, *68* (2), 266−268.
(48) Wan, C.; Zhang, Z.; Woolf, D.; Hessel, C. M.; Rensberg, J.; Hensley, J. M.; Xiao, Y.; Shahsafi, A.; Salman, J.; Richter, S.; Sun, Y.; Qazilbash, M. M.; Schmidt-Grund, R.; Ronning, C.; Ramanathan, S.; Kats, M. A. On the Optical Properties of Thin-Film Vanadium Dioxide from the Visible to the Far Infrared. *Ann. Phys. (Berlin, Ger.)* **2019**, *531* (10), 1900188.
(49) P, A.; Chauhan, Y. S.; Verma, A. High Infrared Reflectance Modulation in VO_2 Films Synthesized on Glass and ITO Coated Glass Substrates using Atmospheric Oxidation of Vanadium. *Opt. Mater.* **2020**, *110*, 110438.
(50) Molnár, J.; Sepsi, Ö.; Erdei, G.; Lenk, S.; Ujhelyi, F.; Menyhárd, A. Modeling of Light Scattering and Haze in Semicrystalline Polymers. *J. Polym. Sci.* **2020**, *58* (13), 1787−1795.
(51) Stojanović, D. B.; Brajović, L.; Obradović, V.; Mijailović, D.; Dramlić, D.; Kojović, A.; Uskoković, P. S. Hybrid Acrylic Nanocomposites with Excellent Transparency and Hardness/Toughness Balance. *Prog. Org. Coat.* **2020**, *139*, 105437.

https://doi.org/10.1021/acsengineeringau.2c00027
ACS Eng. Au 2022, 2, 477−485